Available online at www.sciencedirect.com

ScienceDirect

Procedia CIRP 29 (2015) 354 – 359

www.elsevier.com/locate/procedia

The 22nd CIRP conference on Life Cycle Engineering

Minimization of the energy consumption in motion planning for single-robot tasks

Stefania Pellegrinelli[a,]*, Stefano Borgia[a], Nicola Pedrocchi[a], Enrico Villagrossi[a], Giacomo Bianchi[a], Lorenzo Molinari Tosatti[a]

[a]*Institute of Industrial Technologies and Automation, National Research Council, ITIA-CNR, Via Bassini 15, Milan, 20133, Italy*

* Corresponding author. Tel.: +390223699954; fax: +390223999915. *E-mail address:* stefania.pellegrinelli@itia.cnr.it

Abstract

Recently, the importance of sustainable manufacturing has been widely discussed. The optimization of energy consumption in product manufacture has been deeply analyzed, mainly focusing on the energy directly absorbed by the manufacturing process. On the contrary, this paper focuses on the analysis and optimization of the energy consumption related to auxiliary robotic assembly processes, contributing to the identification of sustainable manufacturing strategies for pick and place robots. It proposes a methodology for the automatic generation of robot trajectories and the sequencing of the robot task, while minimizing the energy consumption. A probabilistic roadmap is created to identify a collision-free and minimum energy consumption trajectory for each couple of feasible tasks. Trajectory power consumption is evaluated exploiting dynamic information coming from the real robot motion planner using a model that takes into account the energy behavior of motors and drives and their operative conditions. A set of generated trajectories is selected, defining the task sequence and minimizing the robot cycle time. The differences between the results deriving by employment of the energy consumption minimization criterion versus time minimization criterion are presented through a simplified case.

Peer-review under responsibility of the scientific committee of The 22nd CIRP conference on Life Cycle Engineering

Keywords: Motion planning; Energy consumption; Optimization

1. Introduction

During the last years, the rapid increase of the energy price together with strictly international and national policies has pointed out the problem of energy efficiency [1], moving companies' awareness from the reduction of the production time to the identification of an optimal trade-off between production time and energy consumption.

Since 1998, the energy consumption in the industrial sector has been reducing. For instance, in the US the manufacturing energy consumption decreased by 17% from 2002 to 2010 [2]. However, an unnecessary use of energy equal to 20-40% may still be found. This percentage is impressive considering a total EU-27 industrial energy use of 324 Mtoe (2004-2005) [3].

According to [4], for many industrial processes, *e.g.* the robotized spot-welding assembly, the consumption can be catalogued as "process energy" or "auxiliary energy". The process energy, generally representing the majority of the consumption, is the energy directly used in the manufacturing of the products, *e.g.* the assembly welding energy. The auxiliary energy is the energy required by the operations that allow the execution of the process, *e.g.* robotic energy consumption. Even if several papers cope with the reduction of the process energy [3], auxiliary energy plays a relevant role and deserves to be studied.

In [5], the relevance of the energy consumption reduction in robotic operations is underlined. The paper deals with the optimal placement of a path in the robot workspace so that the energy consumption is minimized coping with geometric, kinematic and dynamic constraints. [6] provides a methodology able to determine robot velocity and acceleration in order to minimize the energy consumption when moving from a starting point to a target point in a predetermined amount of time. Similarly, in [7], the influence of robot movement parameters on energy consumption is presented, focusing on robot optimal speed, acceleration and

Peer-review under responsibility of the scientific committee of The 22nd CIRP conference on Life Cycle Engineering
doi:10.1016/j.procir.2015.02.174

jerk. A more comprehensive approach can be found in [8] with reference to the automobile industry, where the electrical energy consumed by robotic application is about 8%. In this approach, several strategies to save energy for medium and high payload robot are presented: speed and acceleration variation along the robot path, fly-by trajectories and intelligent management of robot breaks. The same attention to energy saving is presented in [9], where an approach for reducing energy consumption of pick-and-place industrial robot is described. As in the previous approaches, the idea is to reduce the total energy consumption by means of constant time scaling, staring from pre-scheduled trajectories. An evolution of this paper can be found in [10], where the modeling and optimization of energy consumption in cooperative multi-robot is proposed. Specifically, the robots are coordinated through the variation of the velocities and acceleration along predefined path. The task execution sequence changes accordingly to the minimization criterion.

This paper proposes a completely different approach. Indeed, the idea is to allow the selection of the collision-free paths to move from a starting point to a target point that minimizes the energy consumption, while considering technological and geometrical constraints. The modification of the robot velocity and acceleration along all the selected paths is not included in this paper, but represents a future work. Moreover, the paper also take into account the whole robot motion plan, i.e. all the trajectories for the execution of several robot tasks have to be defined. Thus, in this paper, a method able to provide a single-robot motion plan minimizing the comprehensive energy consumption is presented, while taking into account robot cycle time.

The paper is structured as follows: in Section 2 the industrial problem is described; Section 3 presents the methodology, while Section 3.1, 3.2 and 3.3 describe in details the three steps of the approach: trajectory generation, robot dynamic and energy assessment, and task sequencing; in Section 4 the test case is presented and discussed; finally, conclusions and future works are driven in Section 5.

2. Problem statement

The paper focuses on the robot energy consumption in pick-and-place tasks. A task consists in the grabbing or release of an object in a specific position, thus representing a constraint to the robot configuration during the task execution. In such a context, two main problems have to be faced: the definition of collision-free trajectories among the tasks (couples of tasks) and the task execution sequence.

These two problems are interconnected since the execution sequence, apart from existing precedence constraints among the tasks, depends on the trajectories definition. In other words, task sequence may not be completely predefined, *i.e.* the final task sequence has to be optimized taking into account the energy consumption, the required cycle time and possible precedence constraints among the tasks. This optimization may lead to different results, if different trajectories are considered. In such a context, the optimization of the energy consumption and the cycle time generally represent a trade-off [9].

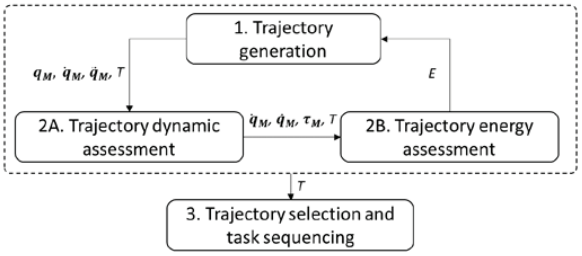

Figure 1: The approach

Worthy, the energy optimization is of upmost importance for pick and place tasks, where only the start and goal configurations are constrained.

3. Methodology

The proposed approach is based on three steps (Fig. 1). The first step (Section 4 - *Step 1*) concerns the generation of the trajectories. Specifically, for each couple of tasks (two tasks that could be executed one after the other), a collision-free trajectory minimizing the energy consumption is defined. The generation of the trajectories exploits the probabilistic roadmap technique [11] and the Open Robot Realistic Library (ORL) [12] provided by COMAU. The ORL library represents the virtualization of the real robot controller, according with the standard RCS [13], providing the robot interpolator and all the functionalities related to the robot dynamic model. The trajectories generated by the ORL are expressed in terms of motor positions q_M, velocities $\dot{q_M}$, and accelerations $\ddot{q_M}$. The minimization of the energy consumption is based on the employment of probabilistic roadmaps that allow the identification of the best geometrical path, along which the joint velocity and the acceleration are maximal.

The evaluation of the energy consumption derives from *Step 2* where the dynamic and energy assessments of the robot trajectory occur. On the basis of the information coming from Step 1, together with the dynamic model of the specific robot and the embedded dynamic parameters, the ORL is responsible of the trajectory dynamic assessment (Section 3.2.1 – *Step 2A*). On the contrary, the trajectory energy consumption E (Section 3.2.2 – *Step 2B*) is provided by an ad-hoc developed model that is able to predict the energy consumption according to the trajectory duration T, velocities $\dot{q}_M$ [rad/s], acceleration $\ddot{q}_M$ [rad/s^2] and torque τ_M [Nm].

The last step of the approach (Section 3.3 - *Step 3*) concerns the definition of the task sequence, thus the selection of the trajectories. Since the cycle time is often a relevant factor, the idea is to define the final sequence selecting the trajectories so that the cycle time is minimized. In such a way, a trade-off between the energy consumption and the cycle time is reached.

3.1. Step 1: Trajectory generation

During trajectory generation, collision-free path has to be calculated within the robot family of tasks. In this activity, three factors have to be considered: the degrees of freedom

(DOF) characterizing the robot, the complexity of the environment and the criterion selected according to which the path is generated and optimized. Indeed, on the one hand, the robot DOF and the environmental complexity lead the technique to be employed; on the other hand, the quality of final trajectory depends by the optimization criterion.

Several methodology addressing the problem of robot motion planning can be found in literature [14], such as potential fields, roadmaps, cell decomposition, probabilistic potential fields, probabilistic roadmaps, probabilistic cell decomposition and simple-query sampling-based method. However, not all the presented methodologies can be successfully employed in high-complex environments with industrial anthropomorphic robot like assembly cells. In such an environment, probabilistic roadmaps seem to be the most promising methodologies [12]. Indeed, this methodology has been successfully exploited to define robot motion planning in body-in-white spot-welding cells [12,15,16].

Concerning the criteria for path optimization, the most common criterion is based on the evolution of the area swept by the robot for reaching the second configuration being in the first configuration [17]. Indeed, the higher the area swept by the robot, the higher the probability to have a collision. In [18,19], different metrics such as the Euclidean, the scaled Euclidean, the Minkowski, the modified Minkowski and the Manhattan distances are evaluated. All the presented metrics are easy to be calculated but are purely geometrical and do not take into account the real industrial problem.

The proposed methodology aims at solving the motion planning for a single robot in a complex environment through the employment of probabilistic roadmaps and an energy consumption minimization criterion.

The idea is to uniformly sample to robot configuration space $C(\mathbf{q})$, with $\mathbf{q}$ the vector of the robot joint coordinates, through Halton point technique [20] and to connect each sampled points to the nearest points. In order to identify the nearest points, the robot energy consumption required to move from the sampled point in analysis to all the other points through joint point-to-point trajectories is evaluated. The trajectories showing the lowest energy consumption determine the nearest points. All the connections are tested for possible collisions with the cell elements [21] to consider only collision-free paths. The generated map is exploited for the identification of the robot minimum energy trajectories between the reference positions of two assembly tasks. The identification of the optimal trajectory is based on the Dijkstra algorithm [22]. At the end, Step 1 provides a minimum-energy and collision-free trajectory for each couple of tasks.

It is important to underline that the generated trajectories are optimal from the energy point of view in relation the specific generated probabilistic roadmap. Thus, a better sampling of the space during roadmap generation will allow the definition of a better energy profile of the trajectories.

3.2. Step 2: Robot Dynamic and Energy Assessment

Commonly, industrial robot is actuated by Permanent Magnet Synchronous Motors PMSM and relative power converters (rectifiers, DC bus and inverter). The robot energy assessment passes through the knowledge of the mechanical power consumption and, thus by the estimation of the motor torque for each robot motor. Section 3.2.1 describes the process leading to the estimation of the motor torque, while Section 3.2.2 present a model for the estimation of the energy consumption taking into account motor torque and losses.

3.2.1. Step 2A: Dynamic Assessment

The joints torques of a standard industrial robot can be calculated by considering the inverse dynamic model of the machine. Starting from the standard rigid multi-bodies dynamic equation, different formulation can be used (*e.g.* the recursive Newton-Euler formulation, or on the Lagrangian energy approach) to write the dynamic equations of the system [23]. By regrouping the analytical equations, the inverse dynamic model of the robot can be written as:

$$\tau_{dyn} = \varphi(q_M, \dot{q}_M, \ddot{q}_M)\pi \tag{1}$$

where, for a manipulator with n DOF, τ_{dyn} is the n x 1 vector of motor torques which includes the contribution of dynamics of the link masses, the first and the second moments of inertia of the link, and the motor rotor inertia. φ is the n x n_p regression matrix (*i.e.* containing all of the geometrical information of the mechanical structure) which is in linear relation with the $n_p x1$ set of dynamic parameters of the machine π, with n_p representing the number of essential parameters obtained from the entire dynamic parameters set as in [24,25]. Finally, the $q_M, \dot{q}_M, \ddot{q}_M$ are respectively the n x 1 joint motor positions, velocities and accelerations vectors.

The friction term contribution can be added as independent term to τ_{dyn}. Different models, with increasing complexity can be considered, but a simple linear model represents a good compromise between accuracy and complexity:

$$\tau_{fricl} = F_v\dot{q} + F_C sign(\dot{q}) \tag{2}$$

where F_v and the F_C are respectively the n x n diagonal matrices representing the viscous and the Coulomb friction parameters.

Thus, the total motor torque τ can be obtained by adding:

$$\tau_M = \tau_{dyn} + \tau_{fricl} \tag{3}$$

The actual values of the dynamics parameters are often not available to the end user, and identification techniques are necessary to extrapolate these values. However, the above-mentioned ORL library that has been used in this work provides directly the calculus of the motor torque. It is worth to underline that the accuracy of the torque estimation given by ORL is guaranteed by the fact the ORL provides the dynamic model integrated in the COMAU robot controller.

3.2.2. Step 2B: Energy Assessment

The main energy consumption is due to the motor. Previous studies assert that PMSM electrical power in robot applications can be estimated by referring to the electrical machine models described in [9,26], which relates the PMSM behavior at a generic operating point with the PMSM behavior at rated (nominal) operation.

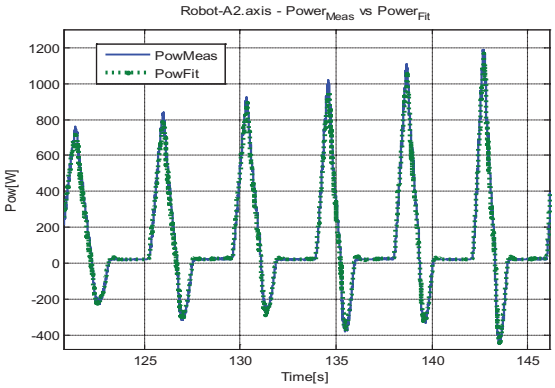

Figure 2: Comparison between measured and estimated power consumption of A2 axis motor during CW and CCW motions.

The selection of the motor model has been led by preliminary experimental investigation using the COMAU NS16-165 [12] robot, which is the robot employed in the test case presented in the Section 4. The experiments have shown that the motors of the robot work always in no flux weakening operative region. Thus, despite many detailed models are presented in literature, *e.g.* based on motor equivalent circuits and on experimental identification of parameters and losses [27,28], a simple model for the motor power losses has been identified. Thus, the motor power absorption P has been modelled as sum of constant power P_B, mechanical power P_M and motor copper losses P_R:

$$P = P_B + P_M + P_R = P_B + k_t\, i_{q\_rms}\, \dot{q}_M + R_S\, i_q^{\,2} \tag{4}$$

where k_t is the motor torque constant [Nm/Arms], i_{q_rms} and i_q are the effective and peak values of the current [A], $\dot{q}_M$ is motor velocity [rad/s], and R_s is the stator resistance [Ω]. So, energy can be obtained as integral of the power along the time.

The estimation of the motor model parameters has been performed through a test campaign consisting of clockwise (CW) and counter clockwise (CCW) motions of each axis of the robot at different velocities and accelerations. Unknown coefficients P_B, k_t and R_s have been estimated using least mean square (LMS) fitting technique (Table 1). The results show a good representation of the power behavior of the axes motors taking as input kinematic and current data provided by robot control (e.g. Fig. 2, power absorption of A2-axis motor). Noteworthy, the validity of the model expressed by Eq. 8 is confirmed by the extremely low values attained by the estimation standard error. Thus, a possible additional term expressing the velocity-dependent losses (*i.e.* iron losses) is not significant in such application scenario and would not improve the power estimation for the considered motors.

As a matter of further validation of this consideration, a spectral analysis has been executed taking into exam 3-phases currents i_1, i_2, i_3 and voltages v_1, v_2, v_3 measured at a sample frequency of 200*kHz*. For each frequency, the motor power P has been computed as follows:

$$P = \mathrm{Re}\{DFT(v_1)\cdot \sim (DFT(i_1)) + DFT(v_2)\cdot \sim (DFT(i_2)) + DFT(v_3)\cdot \sim (DFT(i_3))\} \tag{5}$$

Table 1. Identified parameters for each axis motor.

Parameter	A1	A2	A3	A4	A5	A6
P_B [W]	16.6818	31.2933	16.0939	8.0305	7.8799	8.0009
k_t [Nm/A]	0.5343	0.6083	0.5351	0.2606	0.2451	0.2217
R_s [Ω]	7.1216	2.689	7.1324	2.2807	2.3631	2.8327

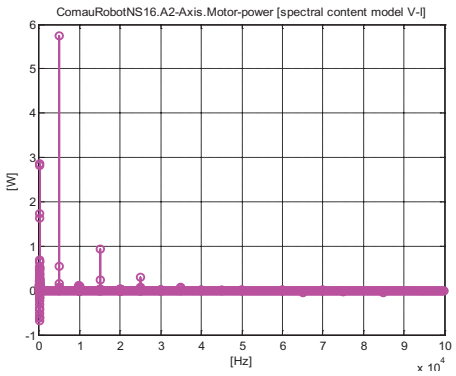

Figure 3: A2-axis motor power spectral analysis.

where DFT is the discrete Fourier transform and ~ is the complex conjugate operator. Power analysis shows at high frequencies the presence of power dissipations due to the pulse with modulation (PWM), represented in the model by the estimated constant power coefficient P_B [W] (Fig. 3). Hence, the analysis results indicate that the below constant current-torque relation is adequate for the application scenario of the here presented work.

$$i_{q\_rms} = \frac{\tau_M}{k_t} \tag{6}$$

3.3. Step 3: Trajectory selection and task sequencing

Step 3 of the methodology aims at selecting the trajectories and fining out the best task sequence so that the robot cycle time is minimized. This can be reduced to the travelling salesman problem (TSP) [29], where the tasks, the trajectories and the trajectories time represent respectively the nodes, the arcs and the arc weights.

The problem is solved through a mixed-integer linear mathematical model, whose indexes, parameters and variables are presented in Table 2, Table 3 and Table 4.

Table 2. Model indexes.

Indexes	Definition
t, t1, t2	Tasks {1,…,*NT*}, where *NT* is the number of tasks to be executed

Table 3. Model Input.

Input	Type	Definition
$FMPf_{t1,t2}$	Bool	Feasible motion plan. Equal to 1 if the robot can execute task *t1* immediately after task *t2*
$MT_{t1,t2}$	Double	Motion time [s]. Time required by the robot for the execution task *t1* immediately after task *t2*
$ME_{t1,t2}$	Double	Motion energy [J]. Energy required by the robot for the execution task *t1* immediately after task *t2*
TT_t	Double	Time required for the execution of the task *t*

Table 4. Model Variable.

Variable		Definition
$MP_{t1,t2}$	Bool	Selected motion plan. Equal to 1 if the robot can execute task *t1* immediately after task *t2*
$MPS_{t1,t2}$	Integer	Task execution sequence. Equal to *k* if the robot can execute task *t1* immediately after task *t2* as k^{th} task.
$S_{t1,t2}$	Double	Instant time in which the robot leaves task *t1* after its execution and approaches task *t2*
$F_{t1,t2}$	Double	Instant time in which the robot approaches the task *t2* after the completion of task *t1*
T_t	Double	Time lap in which the robot moves from task *t1* to task *t2*, and executes *t2*
FEC	Double	Final energy consumption
FCT	Double	Final robot cycle time

The objective function (Eq. 7) aims at minimizing the robot cycle time (*FCT*), while selecting the energy-based previously defined trajectories. Eq. 8 and Eq. 9 impose that from each task *t1*, a single task *t2* is reachable, and each task *t2* is reachable from the task *t2*. Because of the contemporary application of Eq. 8 and Eq. 9, each task can be executed only once. Eq. 10 is necessary to correctly define the optimal task sequence. Eq. 11 assures that, at time step *k*, task *t1* is left for the execution of task *t2* at time step *k+1*. Eq. 12 establishes a relation between the *MP* and *MPS* matrices. Eq. 13-Eq. 16 lead to the definition of the motion plan in terms of initial time and completion time: Eq. 13 defines the initial time of the motion plan, Eq. 14 imposes the equality among the initial time of a trajectory and the completion time that considers the trajectory duration and the task duration (Eq. 15 and Eq. 16). Eq. 17 determines the equality between FCT and the biggest completion time. Finally, Eq. 18 provides the energy consumption related to the motion plan.

Minimize: FCT (7)

Subject to:

$$\sum_{t1} MP_{t1,t2} = 1 \quad \forall t2 \tag{8}$$

$$\sum_{t2} MP_{t1,t2} = 1 \quad \forall t1 \tag{9}$$

$$\sum_{t2} MPS_{0,t2} = 1 \tag{10}$$

$$\sum_{t2} MPS_{t,t2} - \sum_{t1} MPS_{t1,t} = 1 \quad \forall t \neq 0 \tag{11}$$

$$MP_{t1,t2} \geq \frac{MPS_{t1,t2}}{NT} \quad \forall t1,t2 \tag{12}$$

$$I_{0,t2} = 0 \quad \forall t2 \tag{13}$$

$$\sum_{t2} I_{t,t2} = \sum_{t1} C_{t1,t} \quad \forall t \neq 0 \tag{14}$$

$$C_{t1,t2} = I_{t1,t2} + T_{t1,t2} \quad \forall t1,t2 \tag{15}$$

$$T_{t1,t2} = MP_{t1,t2} MT_{t1,t2} + MP_{t1,t2} TT_{t2} \quad \forall t1,t2 \tag{16}$$

$$FCT \geq C_{t1,t2} \quad \forall t1,t2 \tag{17}$$

$$FEC = \sum_{t1,t2} MP_{t1,t2} ME_{t1,t2} \quad \forall t1,t2 \tag{18}$$

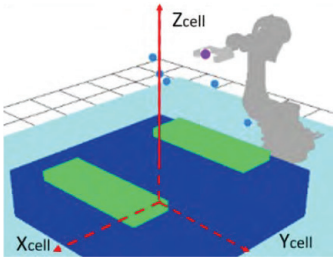

Figure 4: Simplified case

Table 5. Robot position and orientation in the cell.

R1	COMAU NS16-165
Rototranslation - position [mm]	[1 0 0 -2000; 0 1 0 0; 0 0 1 0; 0 0 0 1]
Home joint position [°] – HP	0 0 -90 0 0 0

Table 6. Robot tasks

Task	Position [mm]	ZY'Z'' orientation [°]
T1	-800 -700 1000	30 5 30
T2	-1300 0 600	10 30 10
T3	-450 250 1300	50 40 10
T4	-600 -700 1300	20 10 0
T5	-500 -500 1200	-40 -10 -10

4. Test Case

A pick-and-place test case is hereafter presented and analysed. An anthropomorphic COMAU NS16-165 robot (R1) is employed for the execution of 5 assembly tasks (Fig. 4). The robot position and orientation, its home position (called HP) as well as the task position respect to the cell reference system are described in Table 5 and Table 6. Precedence constraints among the tasks are not considered.

The proposed case is solved according to the paper presented in this approach. The results (S1) are compared with the results obtained by the same approach substituting the energy consumption criterion with the time criterion (S2).

The first experiment (S1) based on the proposed approach led to the identification of a work cycle characterized by a cycle time of 22.7*s* and an energy consumption of 22.27*kJ* with the task sequence HP→T4→T5→T3→T2→T1→HP. On the contrary, the experiment S2 provided a cycle time of 17.98*s* with and energy consumption of 25.19*kJ* and the task sequence HP→T5→T4→T3→T1→T2→HP. Thus, an improvement of 12% on the total energy consumption is reached. Two trajectories can be found in Fig. 5.

A detailed analysis of the most significant results is presented in Table 7. An initial comparison between the results provided by S1 and S2 revels a medium improvement of the energy consumption in S1 by 8% (0.35*kJ*) against a time increase of 38% (0.85*s*). The overall mean is calculated considering all the generated trajectories and not only the subgroup presented in the table. In the majority of the cases, the trajectory energy consumption obtained by S1 is lower that the energy consumption provided by S2. The remaining cases may be explained through the under sampling of the robot joint space during the generation of the probabilistic roadmap. In the best case (trajectory HP-T1), the energy consumption reduction is equal to 59%, i.e. 2.661*kJ*.

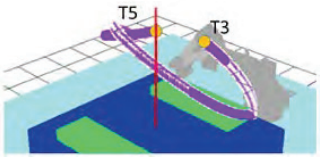

(a) Energy minimization S1 – T3-T5

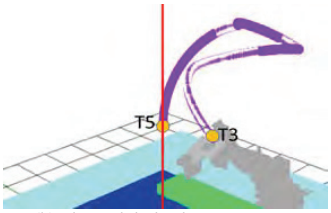

(b) Time minimization S2 – T3-T5

Figure 5: Example of the same trajectory (at the end effector) generated in S1 and S2

Table 7. Detailed results

Trajectory	Energy min – S1		Time min – S2	
	Time[s]	Energy[kJ]	Time[s]	Energy[kJ]
HP-T1	2.72	1.847	2.76	4.508
HP-T2	2.96	2.957	2.55	5.1877
HP-T3	3.26	3.339	2.90	5.509
T1-T2	2.43	2.175	1.39	2.087
T4-T5	3.14	4.836	2.77	5.851
Overall Mean	3.11	4.093	2.26	4.441

The results presented in this section are derived by simulation through the use of a developed software tool. This software tool exploits the experimental parameters of Table 1 for trajectory energy estimation.

5. Conclusions and future work

In this paper, the reduction of the energy consumption related to auxiliary process and specifically to robot energy consumption in pick-and-place operations has been investigated. An approach for the automatic generation of collision-free trajectories minimizing the energy consumption and looking at the robot cycle time has been provided. The developed approach led in the proposed case to the reduction of the work cycle energy by 12%, in comparison to an approach only minimizing the cycle time.

Future work will be related to the analysis of the approach response in a complex and real environment. Moreover, multi-robot motion planning will be taken into account.

Acknowledgements

This paper has been partially funded by Regione Lombardia under the project “Fabbrica intelligente per la deproduzione avanzata sostenibile” (FIDEAS).

References

[1] Unander, F. Decomposition of manufacturign energy use in IEA countries, How do recent development compare with historical long-term trandes, Apllied Energy 84, 2007.
[2] http://www.eia.gov/consumption/manufacturing, visited on Dec. 2014.
[3] Fysikopoulos, A., et al.. An Empirical Study of the Energy Consumption in Automotive Assembly. Procedia CIRP, 3, 477–482, 2012.
[4] Neugebauer, R., Putz, M., Böhme, J., Todtermuschke, M., & Pfeifer, M. Sustainable Manufacturing, 197–201. 2012.
[5] Ur-Rehman, R., Caro, S., Chablat, D., & Wenger, P. (2009). Path placement optimization of manipulators based on energy consumption: application to the orthoglide 3-axis.
[6] Bryan, C., Grenwalt, M., & Stienecker, A. Energy Consumption Reduction in Industrial Robots. In ASEE Conference (pp. 1–4). Pittsburgh, PA, 2010
[7] Smetanová, A. Optimization of energy by robot movement. MM Science Journal, (March), pp. 172–173, 2010.
[8] Meike, D., & Ribickis, P. L. Analysis of the Energy Efficient Usage Methods of Medium and High Payload Industrial Robots in the Automobile Industry. In 10th Int. Symp. “Topical Problems in the Field of Electrical and Power Engineering” (pp. 62–66). Estonia, Jan 2010.
[9] Pellicciari, M., G.Berselli, F.Leali, & A.Vergnano. A method for reducing the energy consumption of pick-and-place industrial robots. Mechatronics, 23, 326–334, 2013.
[10] Vergnano, A., Lennartson, B., Falkman, P., Pellicciari, M., Leali, F., & Biller, S. Modeling and Optimization of Energy Consumption in Cooperative Multi-Robot Systems. IEEE T-ASE, 9(2), 2012.
[12] Latombe, J.-C. Robot motion planning (Vol. The Spring). United States of America: Kluwer Academic Publishers; 1991.
[12] COMAU S.p.A. COMAU web page. Retrieved from http://www.comau.com. Visited on Dec. 2014.
[13] Realistic Robot Simulation - http://www.realistic-robot-simulation.org. Visited on Dec. 2014.
[14] LaValle, S. M. Planning Algorithms. (Cambridge, Ed.); 2003.
[15] Pellegrinelli, S., Pedrocchi, N., Molinari Tosatti, L., Fischer, A., Tolio, T. Multi-robot spot-welding cells: an integrated approach to cell design and motion planning, CIRP Annals – Manuf Tech, 63(1): 17-20, 2014.
[16] Pellegrinelli, S., Pedrocchi, N., Molinari Tosatti, L., Fischer, A., & Tolio, T. Design and motion planning of body-in-white assembly cells. In IEEE/RSJ Int Conf on Int Rob and Sys. 2014. Chicago, Illinois.
[17] Kavraki, L.E., Svestka, P., Latombe, J.-C., & Overmars, M.H. Probabilistic roadmaps for path planning in high-dimensional configuration spaces. IEEE Tra Automat Contr, Robot and Automat, 12(4):566–580, 1996.
[18] Kuffner, J. J. Effective sampling and distance metrics for 3D rigid body path planning. In IEEE International Conference on Robotics and Automation, Vol. 4, pp. 3993–3998), 2004.
[19] Amato, N. M., et al. Choosing good distance metrics and local planners for probabilistic roadmap methods. IEEE Trans. on Rob. and Aut., 16(4):442–447, 2000.
[20] Geraerts, R., & Overmars, M. A Comparative Study of Probabilistic Roadmap Planners. In J.-D. and B. Boissonnat Joel and Goldberg, Ken and Hutchinson, Seth (Ed.), Algorithmic Foundations of Robotics V, Vol. 7, pp. 43–58. Springer Berlin Heidelberg 2004.
[21] Gottschalk, S., Lin, M. C., & Manocha, D. OBBTree: A Hierarchical Structure for Rapid Interference Detection. SIGGRAPH ’96 Proc of the 23rd Conf on Comp Grap and Inter Tech, pp. 171–180, 1996.
[22] Karaman, S., & Frazzoli, E. Sampling-based algorithms for optimal motion planning. Int. J. of Robotics Research, 30(7), 846–894, 2011.
[23] Siciliano, B., Sciavicco, L., Villani, L., & Oriolo, G. Robotics Modelling, Planning and Control. Springer. 2009. 632p.
[24] Pham, C.M., Gautier, M. Essential parameters fo robots. Decision and control, 1991. Precedeings of the 30th IEEE Conference on, Vol. 3, pp. 12769-2774, 11-13 Dec 1991.
[25] Antonelli, G., Caccavale F. and Chiacchio P. A systematic procedure for the identification of dynamic parameters of robot manipulators. Robotica. pp. 472-435.
[26] Kiel, E. Drive Solutions, Mechatronics for Production and Logistics. New York, NY, USA: Springer, 2008
[27] Morimoto, S., Tong, Y., Takeda, Y. and Hirasa, T. Loss Minimization Control of Permanent Magnet Synchronous Motor Drives. IEEE Transaction on Industrial Electronics, vol.41, no.5, 1994
[28] Mi, C., Slemon, G.R. and Richard Bonert, R. Modeling of Iron Losses of Permanent-Magnet Synchronous Motors. IEEE Trans Ind Applic, Vol.39, no.3, 2003
[29] B. Gavish, S.C. Graves, The travelling Salesman Problem and Related Problems, Working Papers OR-078-78, MIT, Cambrige, MA, 1978